Gagliardi et al., https://doi.org/10.1083/jcb.201703044

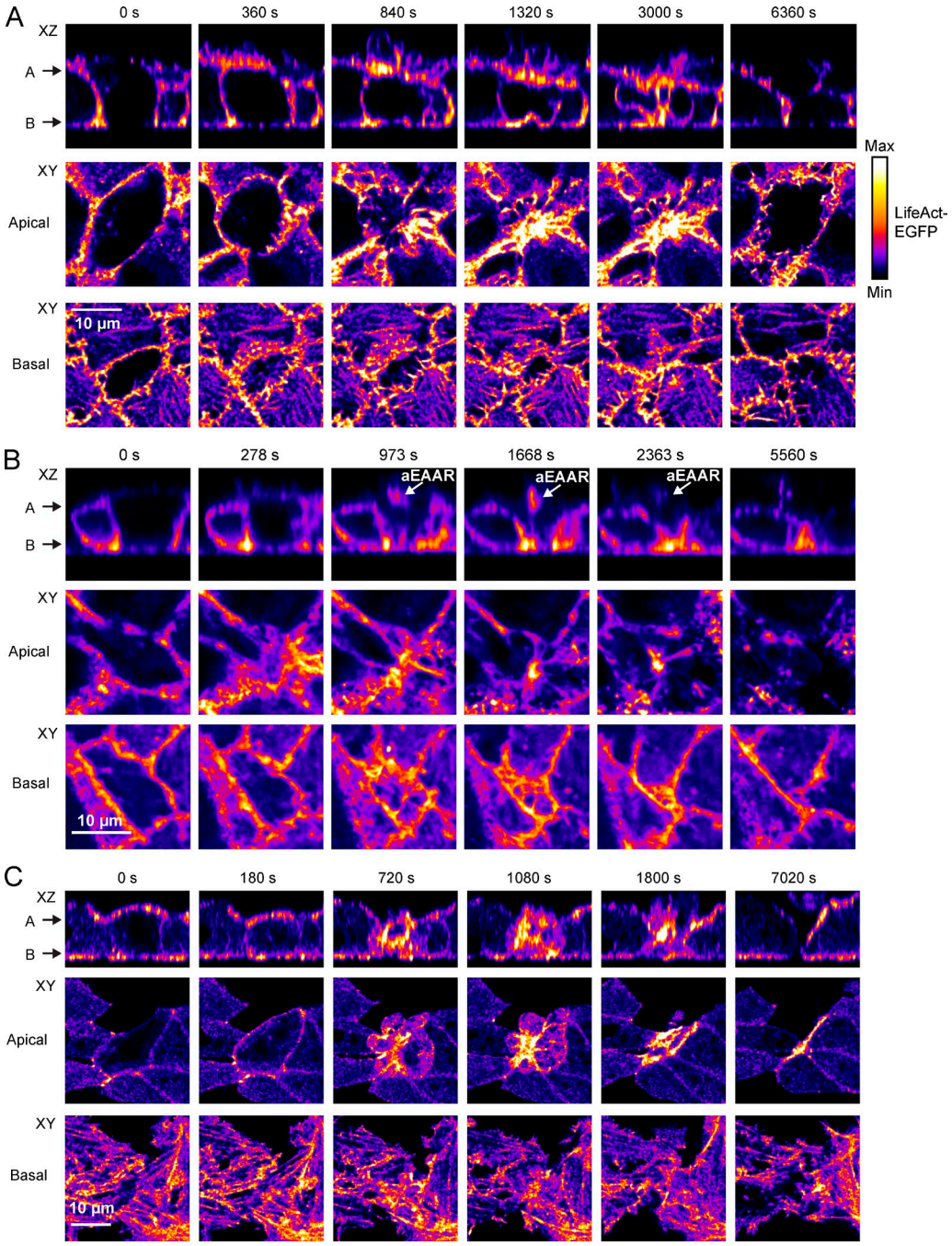

Figure S1. **aEAAR is observed during apoptotic epithelial extrusion. (A and B)** MCF10A cells, stably transduced with LifeAct-GFP, were cultured as a confluent layer in growth medium, and then serum and growth factors were removed to stimulate cell extrusion. **(C)** MDCK cells, stably expressing LifeAct-GFP, were cultured until confluence in medium supplemented with serum. Then serum was removed to induce spontaneous event of extrusion. The image sequences show an *XZ* section and *XY* sections at apical and basal sides of cells imaged during cell extrusion.

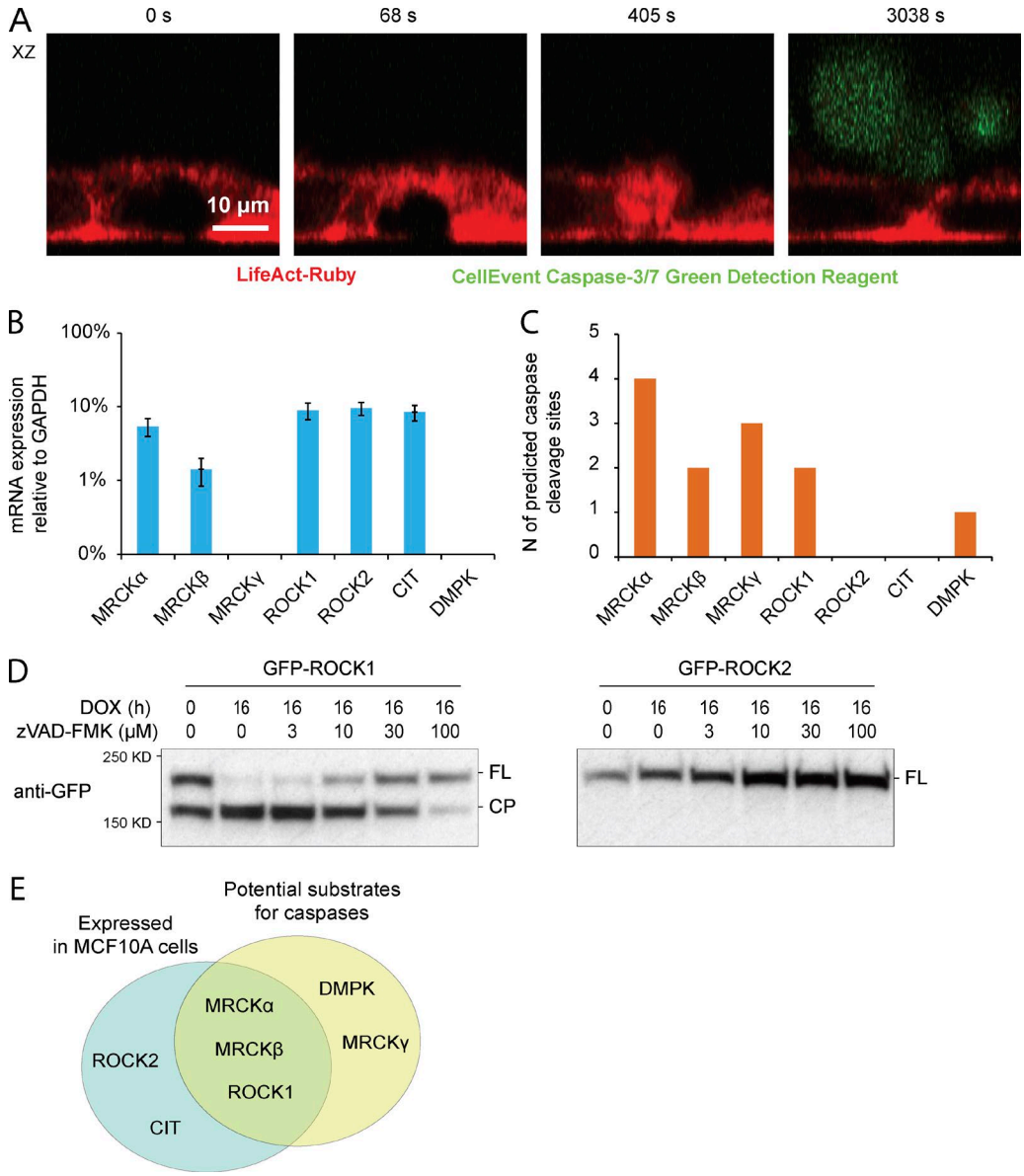

Figure S2. **Study of Rho GTPase–associated kinase family to discover mediators of epithelial cell extrusion. (A)** MCF10A cells were stably transduced with LifeAct-Ruby, and epithelial extrusion was induced in presence of the live caspase marker CellEvent Caspase-3/7 Green Detection Reagent (Thermo Fisher Scientific) that accumulates green fluorescent signal into the nucleus after caspase-mediated proteolytic cleavage. **(B)** Gene expression analysis of MRCKα, MRCKβ, MRCKγ, ROCK1, ROCK2, CIT, and DMPK in MCF10A was performed by real-time quantitative PCR, and expression data are reported in relation to GAPDH expression. Error bars represent the SD. **(C)** In silico analysis for putative cleavage sites in MRCKα, MRCKβ, MRCKγ, ROCK1, ROCK2, CIT, and DMPK. The *y*-axis indicates the number of sites having both >0.7 probability of cleavage according to ScreenCap3 and >0.5 probability of random loop obtained by GOR IV method (see Materials and methods). **(D)** GFP-ROCK1 and GFP-ROCK2 were expressed in HeLa cells, and cells were treated with 25 µM of the apoptosis inducer doxorubicin. Caspase-mediated cleavage of ROCK1 was inhibited by growing concentrations of the caspase inhibitor zVAD-FMK. Efficiency of caspase cleavage was detected by evaluating the presence of a cleavage product (CP) in comparison to full-length (FL) protein by immunoblotting with anti-GFP antibody. **(E)** For further analysis, we selected three of seven Rho-associated kinases that match both expression and in silico cleavage criteria.

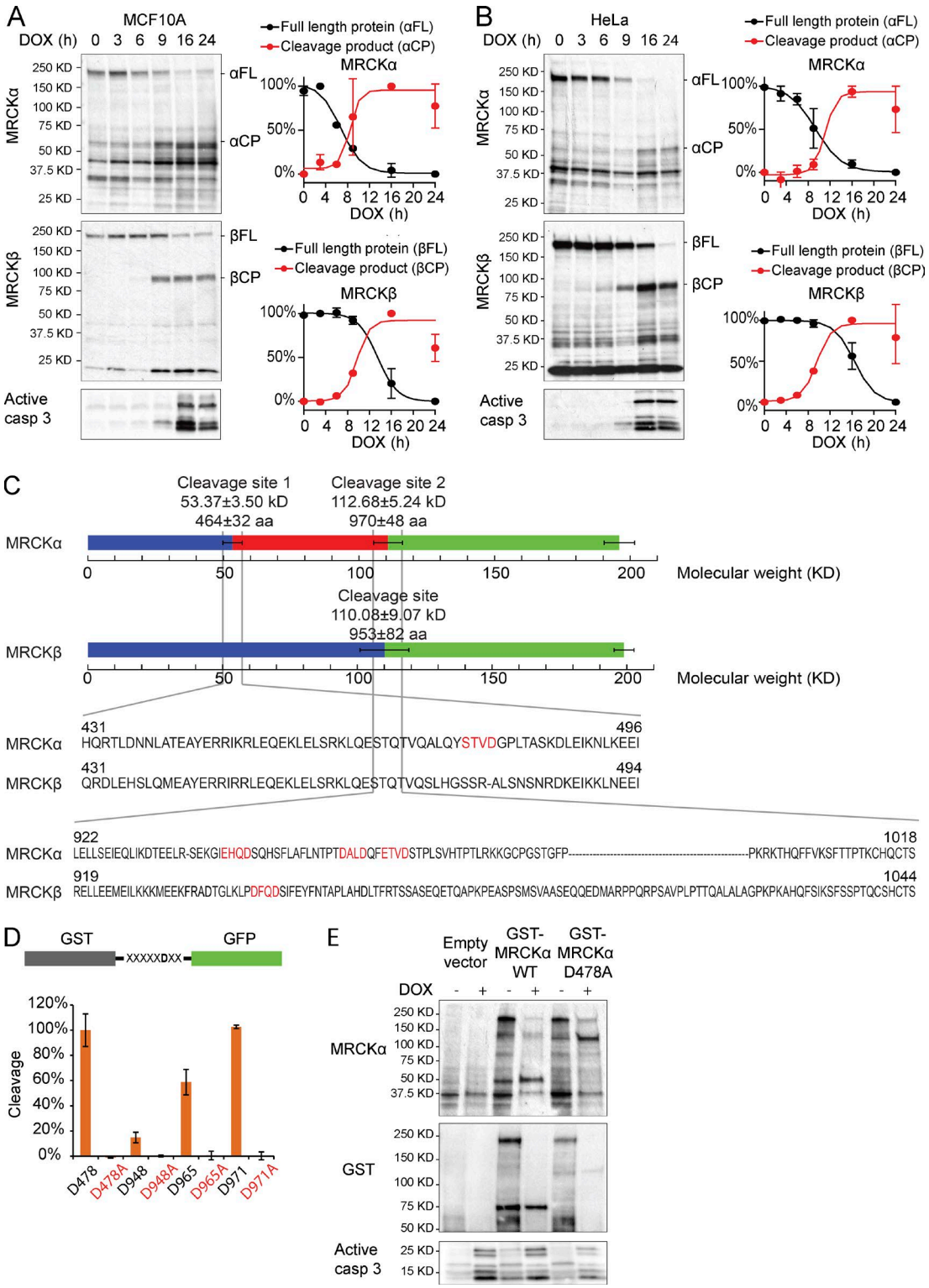

Figure S3. **MRCKα and MRCKβ are cleaved by caspases during apoptosis. (A)** MCF10A cells were treated with 10 μM doxorubicin for the indicated number of hours and lysed. Induction of apoptosis was evaluated by the antibody recognizing cleaved caspase 3. MRCKα and MRCKβ cleavage during apoptosis was evaluated by means of two monoclonal antibodies. Representative immunoblots are reported on the left, and band quantification in multiple experiments is reported on the right. **(B)** The same experiment as in A was conducted in HeLa cells treated with 25 μM doxorubicin. **(C)** Identification of the cleavage sites in MRCKα and MRCKβ. Error bars represent SD according to multiple measures of electrophoretic band migration length. Reported sequences are those included between +SD and −SD of MRCKα and MRCKβ cleavage sites. **(D)** Cleavage screening of putative caspase-substrate sequences in sites 1 and 2 of MRCKα. As negative controls, all the aspartates have been mutated in Ala and compared in the same assay. Proteolytic cleavage was evaluated by immunoblot using anti-GST and anti-GFP antibodies. Cleavage efficiency was evaluated by measuring mean band intensity of the cleavage product and normalized with the cleavage product of D478 construct. In all the experiments, error bars represent the SD. **(E)** HeLa cells knocked out for MRCKα were transiently transduced with GST-MRCKα WT and GST-MRCKα D478A. Apoptosis was induced by 25 μM doxorubicin and verified by immunoblot detecting cleaved caspase 3. GST-MRCKα cleavage was detected by MRCKα monoclonal antibody and anti-GST antibody.

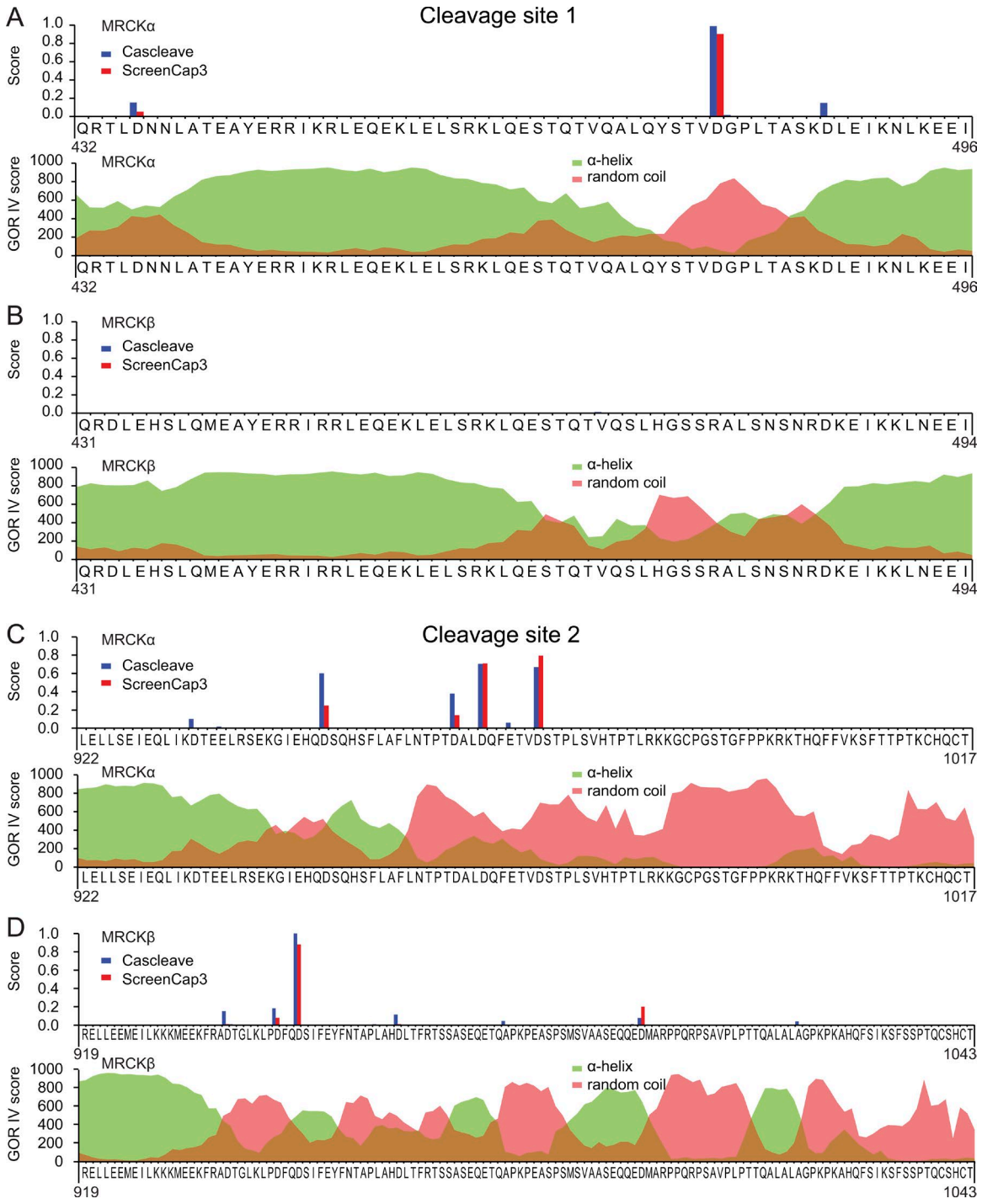

Figure S4. **In silico analysis of first and second cleavage sites in MRCKα and the paralogue sequences in MRCKβ. (A)** The amino acid sequence included between ±SD of the first cleavage site in MRCKα was analyzed for cleavage probability by means of ScreenCap3 webserver and Cascleave webserver (top). The same sequence was analyzed for probability of α-helix secondary structure and random loops (bottom) using GOR IV method. **(B)** The same analysis as in A was conducted on the homologous sequence in MRCKβ. **(C)** The amino acid sequence included between +SD and −SD of the second cleavage site in MRCKα was analyzed as in A. **(D)** The same analysis as in C was conducted on the homologous sequence in MRCKβ.

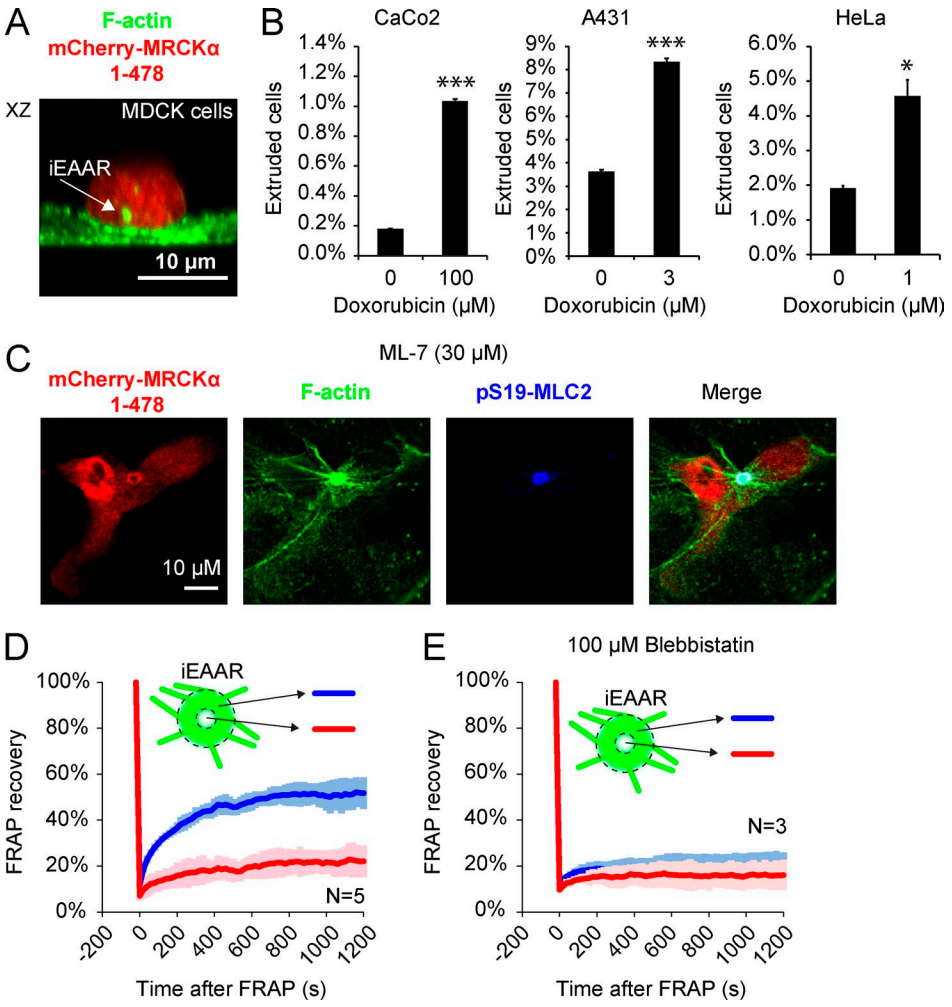

Figure S5. **Epithelial extrusion in other cell lines and iEAAR dynamics. (A)** mCherry-MRCKα 1–478 expression in MDCK cells triggers iEAAR assembly and epithelial extrusion. **(B)** Apoptotic epithelial extrusion is induced in HeLa, Caco2, and A431 by 1, 100, and 3 μM doxorubicin, respectively. Error bars represent ± SD of representative experiment (results confirmed in $n = 3$ independent experiments). *, $P < 0.05$; ***, $P < 0.001$. **(C)** MCF10A cells were transduced with mCherry-MRCKα 1–478 in the presence of the MLCK inhibitor ML-7. Staining for F-actin and phosphorylated MLC2 demonstrates that MRCK induces iEAAR formation independently from MLCK. **(D)** Bleaching experiment of iEAAR in a cells cotransfected with GFP-actin and mCherry-MRCKα 1–478. Fluorescence recovery was measured in the outer and inner regions of the iEAAR. **(E)** The experiment shown in C was repeated in presence of 100 μM blebbistatin and evaluated in the same way. Dark lines represent the mean values, and light shades represent the area included between +SD and −SD.

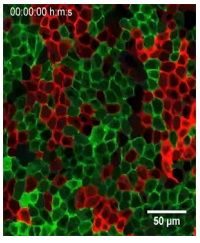

Video 1. **Induction of epithelial extrusion in a confluent MCF10A epithelial layer by removal of growth factors.** Related to Fig. 1 A. Mammary epithelial MCF10A cells stably transduced with LifeAct-GFP or LifeAct-Ruby were mixed at a 1:1 ratio and cultured until confluence. Cell extrusion was induced by deprivation of serum and growth factors. The movie shows a time-lapse experiment of a middle-height *XY* optical section by laser scanning confocal microscopy.

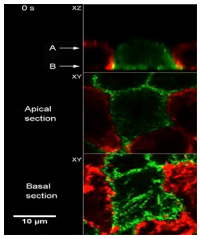

Video 2. **Observation of a cell autonomous apical actin ring (aEAAR) in an extruding cell.** Related to Fig. 1 A. Mammary epithelial MCF10A cells stably transduced with LifeAct-GFP or LifeAct-Ruby were mixed at a 1:1 ratio and cultured until confluence. Cell extrusion was induced by deprivation of growth factors. Cells were imaged by laser scanning confocal microscopy. Top window, *XZ* view; middle window, *XY* view at the apical side; bottom window, *XY* view at the basal side.

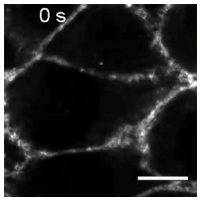

Video 3. **aEAAR assembly is a multistep process.** Related to Fig. 1 C. Mammary epithelial MCF10A cells stably transduced with LifeAct-GFP were cultured until confluence. Cell extrusion was induced by deprivation of growth factors. The movie shows an *XY* optical section of aEAAR assembly in an extruding cell.

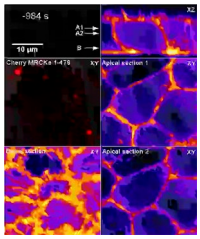

Video 4. **Expression of MRCKα cleavage product in epithelial cells induces iEAAR assembly.** Related to Fig. 4 A. MCF10A cells stably expressing LifeAct-GFP were transiently transfected with mCherry-MRCKα 1–478. The movie shows a cell in which mCherry-MRCKα 1–478 expression and iEAAR assembly are simultaneous events. Top right window, *XZ* view; middle right window, *XY* view at *Z* = A1; bottom right window, *XY* view at *Z* = A2; bottom left window, *XY* view at the basal side; middle left window, *Z* maximum projection of the mCherry-MRCKα channel.

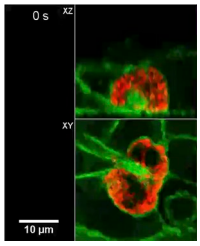

Video 5. **Expression of mCherry-MRCKα 1–478 causes cell extrusion.** Related to Fig. 5 B. The movie shows a MCF10A cell undergoing epithelial extrusion induced by the expression of mCherry-MRCKα 1–478. This cell was part of a confluent MCF10A layer stably expressing LifeAct-GFP. Top window, *XZ* view; bottom window, *XY* view at midheight position.

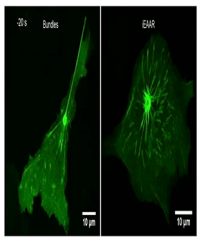

Video 6. **F-actin dynamics in the iEAAR/bundles network.** Related to Fig. 7 (E and J). MCF10A cells were cotransfected with GFP-actin and mCherry-MRCKα 1–478. Then, actin bundles (left) or the iEAAR (right) were bleached to follow the movements of F-actin within the iEAAR/bundles network.

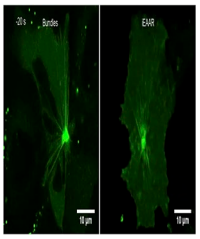

Video 7. **Myosin inhibition impairs actin bundles' flow and F-actin dynamics within the iEAAR.** Related to Fig. 8 (G and H). Cells were cotransfected with GFP-actin and mCherry-MRCKα 1–478. Upon iEAAR assembly completion, cells were treated with 100 µM blebbistatin, and 10 min later, actin bundles (left) or the iEAAR (right) were bleached and monitored by time-lapse laser scanning confocal microscopy.

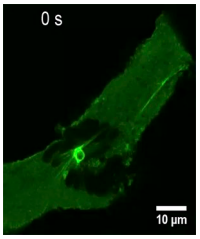

Video 8. **iEAAR/bundle network dynamics is characterized by tug-of-war and collapse phases.** Related to Fig. 9 A. The image sequence shows a MCF10A cell expressing GFP-actin and mCherry-MRCKα 1–478 and followed until collapse. In the tug-of-war phase, the cell is subjected to limited morphological changes. The collapse phase instead can be recognized by a rapid shortening of iEAAR-associated bundles.

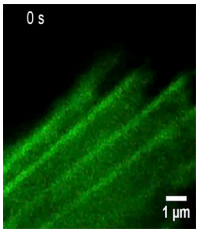

Video 9. **Actin polymerization is observed at iEAAR bundles' terminals.** Related to Fig. 9 D. MCF10A cells were cotransfected with GFP-actin and mCherry-MRCKα 1–478, photobleached at the outermost terminals of iEAAR-associated bundles, and recorded by time-lapse confocal microscopy.

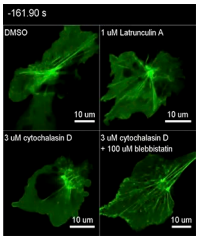

Video 10. **Impairment of actin polymerization causes rapid iEAAR/bundle structure collapse and cell contraction.** Related to Fig. 9 F. Cells were cotransfected with GFP-actin and mCherry-MRCKα 1–478 and, after iEAAR assembly, treated with 1 µM latrunculin A, 3 µM cytochalasin D, or cotreated with 100 µM blebbistatin and 3 µM cytochalasin D. Block of actin polymerization causes sudden shortening of bundles and cell collapse. This collapse is mediated by myosin contraction and is impaired by the simultaneous inhibition of myosin.